Research Article
doi.org/10.1002/cbic.202300369
Chemistry Europe
European Chemical Societies Publishing

www.chembiochem.org

# Establishment of an In Bacterio Assay for the Assessment of Carbon Storage Regulator A (CsrA) Inhibitors

Yingwen Wu,[a, f] Ben G. E. Zoller,[a] Mohamed Ashraf Mostafa Kamal,[b, c] Sven-Kevin Hotop,[d] Claus-Michael Lehr,[b, c] Mark Brönstrup,[d] Petra Dersch,[e] and Martin Empting*[a, c, f]

Polymicrobial infections involving various combinations of microorganisms, such as *Escherichia*, *Pseudomonas*, or *Yersinia*, can lead to acute and chronic diseases in for example the gastrointestinal and respiratory tracts. Our aim is to modulate microbial communities by targeting the posttranscriptional regulator system called carbon storage regulator A (CsrA) (or also repressor of secondary metabolites (RsmA)). In previous studies, we identified easily accessible CsrA binding scaffolds and macrocyclic CsrA binding peptides through biophysical screening and phage display technology. However, due to the lack of an appropriate *in bacterio* assay to evaluate the cellular effects of these inhibitor hits, the focus of the present study is to establish an *in bacterio* assay capable of probing and quantifying the impact on CsrA-regulated cellular mechanisms. We have successfully developed an assay based on a luciferase reporter gene assay, which in combination with a qPCR expression gene assay, allows for the monitoring of expression levels of different downstream targets of CsrA. The chaperone protein CesT was used as a suitable positive control for the assay, and in time-dependent experiments, we observed a CesT-mediated increase in bioluminescence over time. By this means, the cellular on-target effects of non-bactericidal/non-bacteriostatic virulence modulating compounds targeting CsrA/RsmA can be evaluated.

## Introduction

Antimicrobial resistance (AMR) is a concerning worldwide health issue and inappropriate infection prevention and control is one factor for the steadily increasing occurrence of resistant microbes.[1] Without any counteractions, the spread of AMR will assumedly result in the deaths of 10 million people per year globally by 2050.[1]

Addressing and combatting AMR is very challenging, especially considering Gram-negative multi-drug-resistant (MDR) pathogens. Along these lines, carbapenem-resistant *Acinetobacter baumannii*, *Pseudomonas aeruginosa*, and *Enterobacteriaceae* are the top three on the WHO global priority pathogens list published in 2017.[2] Antibiotics or anti-infectives with alternative modes-of-action against these bacteria are therefore urgently needed.

In general, a healthy human microbiome contains diverse communities of microbes, which are stable and provide protection against colonization by pathogenic species. To suppress the growth of pathogens, commensal bacteria produce their own antimicrobial compounds such as peptides.[3] Dysbiotic communities, on the contrary, are typically less diverse and more dominated by few pathogenic species. These interactions lead to polymicrobial infections and in case these microbes are pathogenic, this can enhance the virulence of each of them. There are several examples of this effect including inhibition of competing microbes (so-called microbial interference), the mutual supply of nutrients in particular carbon sources, or subversion of immunity.[3–5]

Many acute and chronic diseases are associated with infections of the respiratory and gastrointestinal tract, where polymicrobial interactions are paramount.[4] Impacting and modulating these complex communities in order to reestablish or protect the commensal balance by small molecular entities might provide an attractive new approach for the discovery of anti-infectives. In this context, the CsrA (RsmA) protein could be considered a promising drug target. The Csr (carbon storage regulator) or Rsm (regulator of secondary metabolites) system is a post-transcriptional regulatory system, which affects mRNA

[a] *Y. Wu, B. G. E. Zoller, Dr. M. Empting*
*Department of Antiviral & Antivirulence Drugs (AVID)*
*Helmholtz Institute for Pharmaceutical Research Saarland (HIPS)*
*Saarland University, 66123 Saarbrücken (Germany)*
*E-mail: martin.empting@helmholtz-hips.de*

[b] *M. A. M. Kamal, Prof. Dr. C.-M. Lehr*
*Department of Drug Delivery (DDEL)*
*Helmholtz Institute for Pharmaceutical Research Saarland (HIPS)*
*Saarland University, 66123 Saarbrücken (Germany)*

[c] *M. A. M. Kamal, Prof. Dr. C.-M. Lehr, Dr. M. Empting*
*Department of Pharmacy*
*Saarland University, 66123 Saarbrücken (Germany)*

[d] *Dr. S.-K. Hotop, Prof. Dr. M. Brönstrup*
*Department of Chemical Biology*
*Helmholtz Centre for Infection Research*
*German Center for Infection Research (DZIF)*
*38124 Braunschweig (Germany)*

[e] *Prof. Dr. P. Dersch*
*Institute of Infectiology*
*Center for Molecular Biology of Inflammation (ZMBE)*
*University of Münster, 48149 Münster (Germany)*

[f] *Y. Wu, Dr. M. Empting*
*Cluster of Excellence RESIST (EXC 2155), Hanover Medical School*
*Carl-Neuberg-Straße 1, 30625 Hanover (Germany)*

*Supporting information for this article is available on the WWW under https://doi.org/10.1002/cbic.202300369*

translation and/or stability, thereby regulating a multitude of cellular processes in response to environmental cues.[6–9] CsrA (RsmA) is a homodimer with two identical RNA-binding surfaces, which recognizes and binds to the GGA motifs in mRNAs. This highly conserved RNA-binding protein is widespread among Gram-negative pathogens.[6–10] For example the homology between CsrA from *Y. pseudotuberculosis* and CsrA from *E. coli* is 95%.[6] CsrA homologs can also be found in a variety of bacterial animal and plant pathogens.[6]

Early evidence showed that CsrA is not only essential for fundamental physiological properties and metabolism, but also for regulation of virulence factors required for host infection.[6] This was confirmed in previous studies by weakened virulence in murine models of e.g. *Y. pseudotuberculosis* using CsrA knock-out strains.[6,7] CsrA's activity includes for example modulation of carbon metabolism, motility, biofilm development, and quorum sensing.[7–11]

## Regulation of Csr system

The complex regulation circuits of the Csr system of *E. coli* have been described in detail in reviews.[9,10] To illustrate the composition and function of the system, a simplified version is shown in Figure 1 including the essential steps relevant for the present study. In the following, the innate antagonists of CsrA will be described more in detail.

The activity of CsrA is controlled by the sequestration of the inhibitory sRNAs CsrB and CsrC (~350 nt long). Furthermore, the amount of CsrB and CsrC determines the level of free, functional CsrA, which is available for binding target mRNAs. The reason for the considered high affinity towards CsrB is for example the existence of 22 potential binding sites, which are able to sequester ~9 CsrA dimers (Figure 2). The binding element for CsrA is suggested to be the hairpin loop motif 5'-CA**GGA**UG-3'.[9,10,12] Experiments with △*csrB/C E. coli* strains and *csrB/C* overexpressing strains showed that its absence or increased abundance caused pleiotropic effects on bacterial physiology. Furthermore, expression of downstream targets regulated by CsrA such as *glgC* (responsible for glycogen biosynthesis) gene, and *flhDC* (operon for biosynthesis of flagella) is similarly affected. For example, glycogen accumulation and non-motile appearance of *Yersinia csrA* mutant strain have been observed.[6] Overall the regulatory RNAs allow the bacteria to fine-tune CsrA.[9,10,12]

Apart from the sRNA-mediated antagonism present in most CsrA/RsmA systems, there are some organisms that use innate proteins to modulate the activity of CsrA. For example, in Enteropathogenic *E. coli* (EPEC) a recently identified chaperon protein called CesT (Figure 3) binds to CsrA leading to alterations in virulence and metabolic gene expression.[9,10,13]

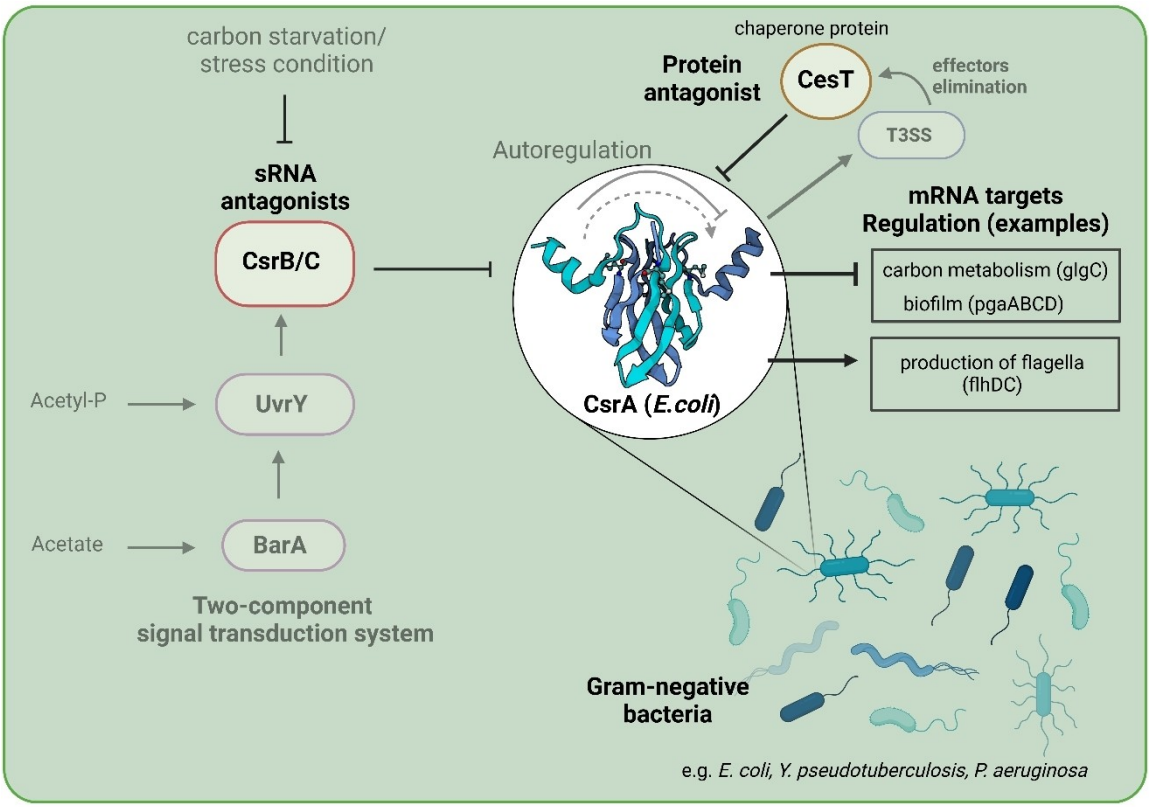


**Figure 1.** Simplified regulation circuit of CsrA in *E. coli*: CsrA is antagonized by sRNAs CsrB/C and chaperone protein CesT. The antagonists are controlled by other feedback cycles and regulatory circuits.[9,10] CsrA itself regulates e.g. the carbon metabolism and biofilm development by repressing the glgC (responsible for glycogen biosynthesis) gene and pgaABCD (operon for biosynthesis and secretion of biofilm polysaccharide adhesin) genes. Furthermore, CsrA activates the expression of flhDC (master operon for flagellum biosynthesis) genes to facilitate the production of flagella.

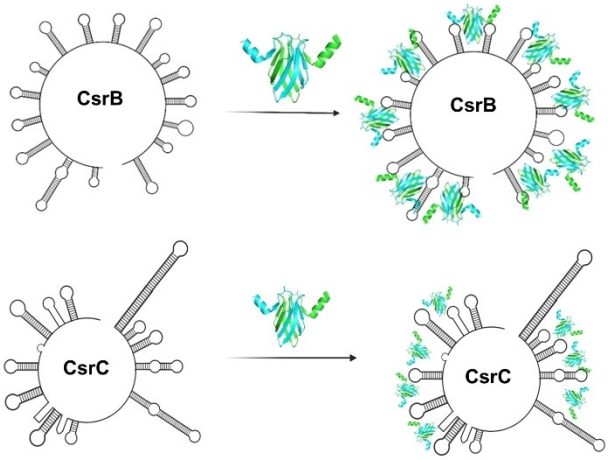


**Figure 2.** sRNA antagonists CsrB and CsrC of CsrA (PDB:1vpz): The affinity of CsrA for CsrB is ~10 fold higher than for CsrC (reported Kd = 8.7 ± 0.6 nM for CsrC) in E. coli,[12] because of the large amount of the binding sites and the co-operative interaction between CsrA and CsrC transcript. Nevertheless, these two sRNAs share a similar mechanism for antagonizing the activity of CsrA. Furthermore, both CsrB and CsrC have a short half-life (~2 min) which indicates that CsrA is able to respond rapidly to changes in CsrB/CsrC levels.[12]

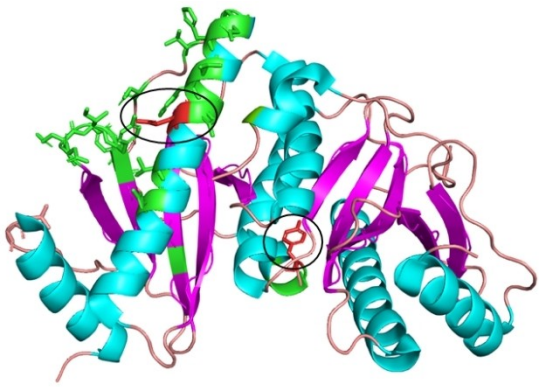

**Figure 3.** Structure of CesT with CsrA binding sites (PDB: 5Z38). CesT is a dimeric protein and one monomer consists of 5 β-sheets (magenta); 3 α-helices (cyan) and loops are shown in salmon. CsrA binding regions are highlighted in green and located mainly at the C-terminal region. Tyr152 and Glu121 are the important binding residues highlighted in red and encircled.[13,14]

The function of CesT is to stabilize and translocate virulence factors (effectors) that are secreted by the type three secretion system (T3SS) and are required for pathogenicity and survival in the host environment.[9,13,14] Furthermore, previous studies showed that during a T3SS-mediated bacterial infection, free CesT (not bound to T3SS effector proteins) binds to the CsrA regulator after injecting the effectors into the host cells. This results in the repression of CsrA-dependent T3SS proteins, which leads to a decrease in T3SS activity and an accumulation of the effectors that sequester CesT. These findings suggest that CsrA and T3SS activities regulate each other indirectly in a negative-feedback loop (Figure 1), while inhibition of CsrA by exogenic substances should lead to a reduction of T3SS activity.[13,14]

## Development of an in bacterio assay for assessing CsrA inhibition

The aim of previous studies was to find novel inhibitors of CsrA, which are capable to disrupt the CsrA-RNA interaction.[7,8] Until now, some interesting CsrA inhibitor scaffolds have been identified using different biophysical screening methods as well as phage display. The discovered hit structures have been tested in a fluorescence polarization (FP) assay for their ability to replace the RNA from CsrA.[8] One of the most active synthetic compounds, which is a triazole peptide, showed an $IC_{50}$ value in a single-digit micromolar range.[8]

However, the biophysical assay reflects the impact on the protein-RNA interaction in a cell-free setup. Since CsrA is a target for pathoblocker compounds, which ideally lack any bactericidal or bacteriostatic effects, typical antibacterial assays like minimum inhibitory concentration (MIC) assays are not suitable. Finding an appropriate *in bacterio* assay, which enables to probe and quantify the impact on CsrA-regulated cellular mechanisms, is challenging. To this end, we employed a (combination of qPCR and) luminescence-based assay setup towards the establishment of an *in bacterio* CsrA inhibition assay.

## Results and Discussion

To study inhibitory effects on target protein levels in real-time, the bioluminescence of bacterial luciferases can be exploited. These enzymes emit light in the presence of the substrate luciferin (reduced riboflavin phosphate), which is oxidized to a long-chain aldehyde.[15] Expression of the bacterial-derived *luxCDABE* operon leads to cells emitting detectable light at 490 nm. This operon encodes the luciferase (LuxAB) and the substrate-producing enzymes (LuxCDE).[15] For our assay we used a vector (pvBE3) containing the *glgC-luxCDEAB* reporter fusion harboring the entire promoter region of *glgC* (which is negatively regulated by CsrA). As a consequence, in the presence of functional CsrA inhibitors, the bioluminescence signal is expected to increase due to the upregulation of target gene (*glgC*) expression.

In order to evaluate a *glgC-lux*-based assay results, we explored the suitability of the innate antagonists as shown in Figure 1 as control. Since CsrB is the main sRNA antagonist of CsrA in *E. coli*, it was the first positive control that we considered. Using a *lactose*-inducible *csrB* expression plasmid, we induced overexpression of CsrB by IPTG (500 μM) treatment. However, unlike what we expected, the bioluminescence decreased after 4 h incubation time (Figure 4A). To gain a better understanding of this outcome, we compared the transcript levels of the individual Csr components by a qPCR gene expression assay after overexpression of CsrB or CsrC (Figure 4B).

We investigated the level of expression of both sRNAs in different strains 4 h after IPTG induction. We could confirm the successful increase of sRNA levels (in a range between 100 to

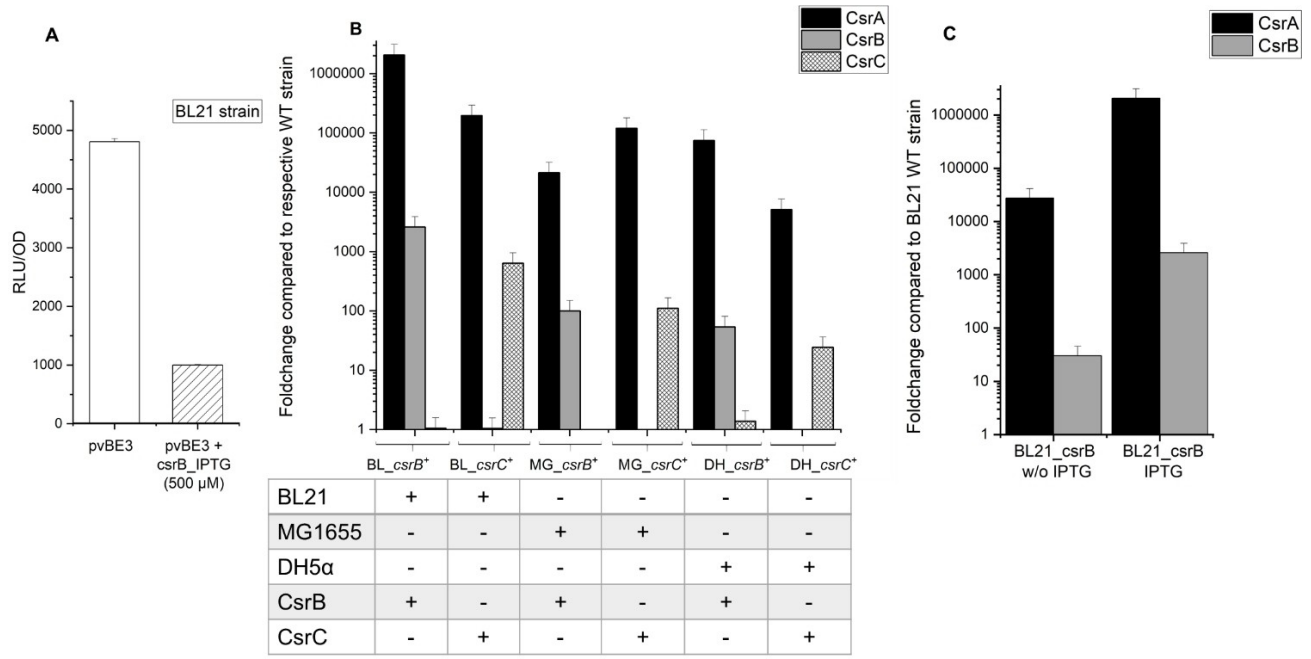


| | | | | | | |
|---|---|---|---|---|---|---|
| BL21 | + | + | - | - | - | - |
| MG1655 | - | - | + | + | - | - |
| DH5α | - | - | - | - | + | + |
| CsrB | + | - | + | - | + | - |
| CsrC | - | + | - | + | - | + |

**Figure 4.** Influence of CsrB overexpression on the luciferase reporter gene (A) and validation of sRNAs' expressions via qPCR assays (B, C). Error bars represent the standard deviation of four replicates. (A): *E. coli* strains BL21 with only the plasmid pvBE3 (*glgC-lux*) or with additional plasmid pET28a(+) harboring the *csrB*$^+$ were grown at 37 °C until the exponential phase was reached (OD = 0.6). The expression of CsrB was induced with 500 µM IPTG. After 4 h of induction the relative light units (RLU) were almost 5-fold less compared to the RLU of pvBE3. All data were normalized over $OD_{600}$. (B): *E. coli* strains BL: BL21 + pvBE3, MG: MG1655 with a constituent T7 promoter + pvBE3, DH: DH5α + pvBE3 with or without the plasmid pET28a(+) (*csrB*$^+$) and (*csrC*$^+$) were grown at 37 °C until exponential phase was reached (OD = 0.6). The wild type strains are mentioned *E. coli* strains without any plasmids. The expression of CsrB or CsrC was induced with 500 µM IPTG. After 4 h of induction with IPTG, total RNA was extracted from the cultures and a qRT-PCR analysis was performed. The results showed that both CsrB and CsrC RNA were increased, but also the expression of CsrA (black bars) was induced to a far greater extent in all strains. C) Results of qPCR expression assay with and without inducing CsrB: *E. coli* strains BL21 pvBE3, with the plasmid pET28a(+) (*csrB*$^+$) were grown at 37 °C until the exponential phase was reached (OD = 0.6). The expression of *csrB* was not induced (w/o) or induced with 500 µM IPTG. After 4 h of induction the relative light units (RLU) were determined. All data were normalized over $OD_{600}$. The basal expression level of *csrA* was higher than in the wild type strain and exceeded the level of CsrB without IPTG. These results suggest that an increased amount of antagonistic sRNAs leads to a feedback mechanism resulting in higher production of CsrA.

3000 fold). However, also CsrA-encoding transcripts were drastically increased (in a range between 5000 to 20.000.000 fold), indicating that CsrB and CsrC overexpression was over-compensated by a 100- to 1000-fold higher *csrA* expression. We further found that strains harboring the *csrB* overexpression plasmid have a significantly higher *csrA* transcript level than in the wild type strain even without IPTG-mediated induction (Figure 4C $p = 0.0128$, calculated using the t-test over the data from BL21 strain harboring csrB without IPTG compared to BL21 strain harboring csrB with IPTG). Ultimately, these qPCR results explained the observation we had from the reporter gene assay.

The results implicated that the induction of sRNA expression triggered an unknown autoregulatory control circuit of the Csr system. Autoregulation of the Csr components has been described, but these studies only report the successful inhibition of the CsrA activity by CsrB/C shown as a *csrA* knock-out phenotype and changes in glucose consumption and free fatty acids production.[16,17] Due to the observed interdependency of the Csr components, using CsrB/C as positive controls proved to be difficult. Therefore, we decided to examine the protein antagonist CesT. This chaperone is reported to inhibit CsrA's activity and should not have an impact on the *csrA* transcript level.[13,14] To ensure that the induction of CesT does not increase CsrA expression, the qPCR gene expression assay described above was applied (Figure 5B). A first observation was, that IPTG addition did not increase *cesT* expression over the basal (uninduced) levels. Importantly, in comparison to the results for CsrB/C, CsrA levels were less, but still affected compared to the wild type in the presence of IPTG (~10-fold), whereas no influence was observed in the absence of IPTG. This effect of the thio-sugar derivative IPTG on *csrA* expression might be linked to the involvement of CsrA in the post-transcriptional control of sugar metabolism.[9,10,17]

The promising results for the *cesT*-harboring plasmid-bearing strain in the absence of IPTG, encouraged us to rely on basal (uninduced) expression in follow-up experiments. We performed the reporter gene assay using the same condition and could observe a convincing increase in bioluminescence, indicating a derepression of the *glgC-lux* fusion in the presence of the *cesT*$^+$ plasmid (Figure 5A). This suggested that the assay setup might be suitable for the identification and investigation of CsrA inhibitors. As a next step, we performed time-resolved experiments to gain insights into the kinetics of CesT-driven inactivation of CsrA in order to identify the most suitable

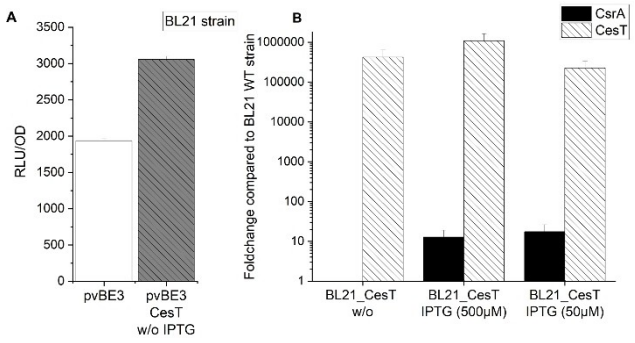


**Figure 5.** Influence of CesT overexpression on the luciferase reporter gene (A) and validation of *cesT* expression on *glgC-lux* transcription by qPCR gene expression assays (B). Error bars represent the standard deviation of four replicates. (A): *E. coli* strains BL21 pvBE3 with or without the plasmid pNS6236 (*cesT*$^+$) were grown at 37 °C until the exponential phase was reached (OD = 0.6) and the relative light units (RLU) were determined. All data were normalized over $OD_{600}$. (B): *E. coli* strains BL21 pvBE3 with or without the plasmid pNS6236 (*cesT*$^+$) were grown at 37 °C until the exponential phase was reached (OD = 0.6). The expression of *cesT* was induced with 50 or 500 µM IPTG. After 4 h of induction with IPTG, total RNA was extracted from the cultures and a qRT-PCR analysis was performed. The presence of the p*cesT*$^+$ had no impact on *csrA* expression in the absence of IPTG.

incubation time for yielding marked effects enabling facile detection of inhibitory activities (Figure 6).

A steady increase of RLU was observed in the *cesT*$^+$ strain BL21 pvEB3, pNS6236 over the course of 5 h, while values of the reference strain BL21 pvBE3 remained essentially unchanged (Figure 6A, also Figure S3). At the end of the five-hour experiment, we determined the most prominent effect, where the RLU of the *cesT*$^+$ strain was ~3-fold higher than the RLU of the control strain. In parallel, we also performed qPCR to monitor the expression levels of *cesT* and *csrA* over the time course of the experiment. The expression level of *csrA* increased 2–40-fold within 2–5 h (Supplementary Figure S2). However, the transcript level of *cesT* was about 10,000-fold higher, and no impact on *glgC-lux* expression has been observed. In order to have enough samples for both assays, we started with a volume of 100 mL culture. However, for efficient compound testing, this large amount of culture is not suitable, because consequently high amounts of potential inhibitors are required. For this reason, we decreased the starting volume from 100 mL over 10 mL down to 200 µL, which was suitable for 96-well format (Figure 6B, C). Results were reproducible. In case of the 10 ml format, the expression patterns looked more defined and the induction of the reporter was more pronounced over time. However, the 200 µL format also yielded well-defined reproducible results clearly enabling to discriminate basal expression from the positive control (Figure 6C). Hence, we consider this assay fit-for-purpose for subsequent compound library screening in the future using the small 96-well plate format.

Based on the data gathered so far, we decided to use 10 mL cultures for the testing of compounds that were previously reported to disrupt the CsrA-RNA interaction in a cell-free environment for the first time.[8] We used disulfide- and triazole-macrocyclized peptidic CsrA inhibitors identified in our previous

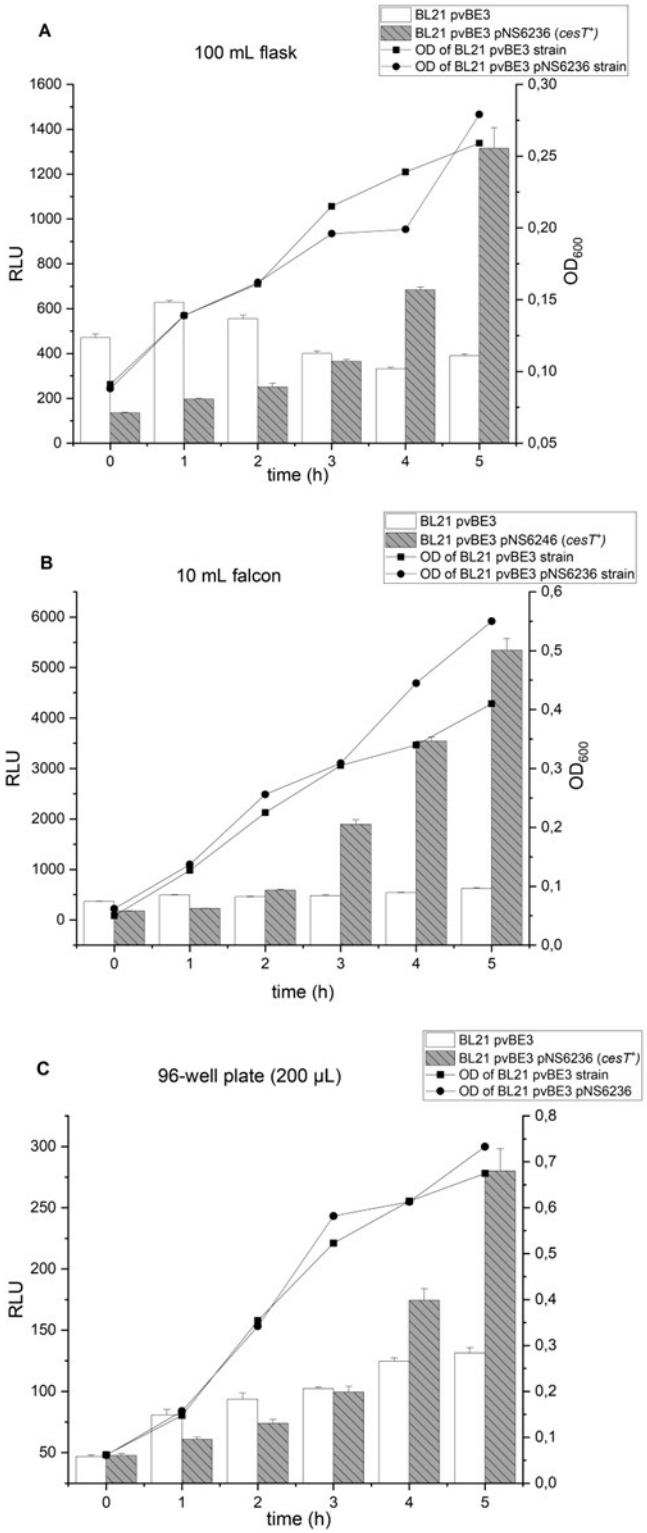


**Figure 6.** Time-dependent reporter gene assay including the positive control CesT and using decreasing assay volumes. Error bars represent the standard deviation of four replicates. (A) 100 ml assay volume run in 300 mL flasks: *E. coli* strains BL21 pvBE3 with or without the plasmid pNS6236 (*cesT*$^+$) were grown at 37 °C for 5 hours and the relative light units (RLU) and OD600 were determined. (B) 10 mL assay volume run in 50 mL falcon tubes. (C) 200 µL assay volume run in 96-well microtiter plates (for details see material and methods section).

study as these were among the most active compounds showing $IC_{50}$ values in a single-digit micromolar range in a fluorescence polarization assay.[8] In contrast to the CesT-expressing positive control, the addition of the inhibitory peptides did not lead to an increase in RLU values, and thus *glgC-lux* expression after 5 hours (Figure 7). We hypothesized that the inability of the peptides to inhibit CsrA in the *in bacterio* assay was due to their difficulty to penetrate the Gram-negative cell membranes and enter the cytoplasm to reach the target protein. This was verified by subcellular quantification of uptake in *E. coli* (supporting information). We observed that the triazole-based peptide **1** reached only nanomolar levels in the cytoplasm, although an extracellular concentration of 28 μM was applied (Figure S4). The intracellular concentrations were clearly insufficient to disrupt the CsrA-RNA interaction given the micromolar potency of the peptide in the target-based assay.

Nevertheless, we consider the general reporter gene assay concept now fit-for-purpose to facilitate quantitative compound evaluation with the aim to identify novel inhibitors with cellular efficacy.

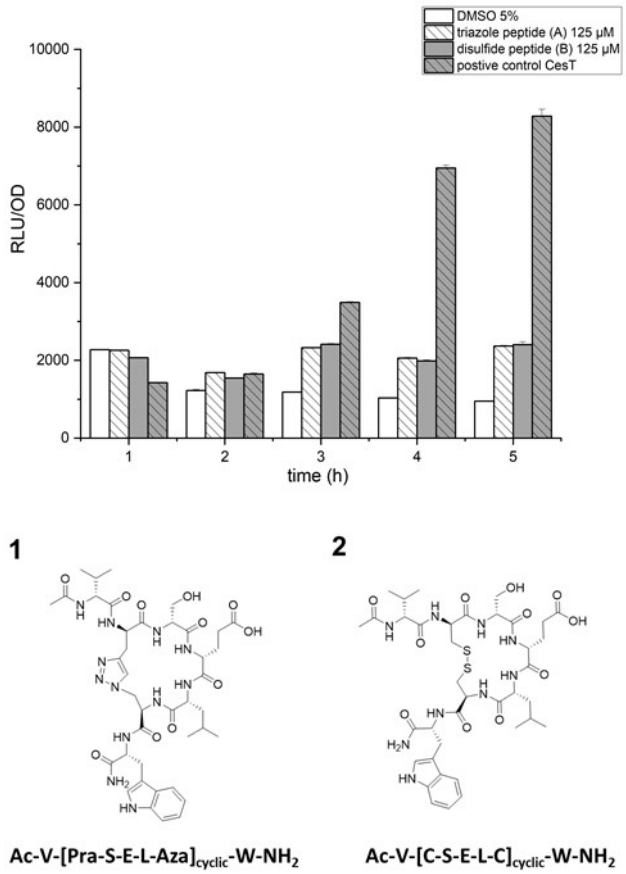


**Figure 7.** Influence of peptidic CsrA inhibitors on the expression of the CsrA-dependent *glgC-lux* fusion: *E. coli* strain BL21 pvBE3 in the presence of 5% DMSO,125 μM triazole peptide **1**, 125 μM disulfide peptide **2** or the plasmid pNS6236 (*cesT*$^{+}$) were grown at 37 °C for 5 hours and the relative light units (RLU) were determined each hour. Error bars represent the standard deviation of four replicates.

## Conclusions

In summary, we could establish an *in bacterio* assay, which directly measures the inhibition of CsrA based on a luciferase reporter gene assay. We could show that the expression of the chaperone protein CesT can be used as a suitable positive control for the assay because it acts as a natural intracellularly expressed antagonist of CsrA, which does not cause compensatory feedback effects. We could monitor a CesT-mediated increase of the bioluminescence over time with the most convincing effect being detectable after 5 hours of incubation.

Another interesting finding from our study is the enhancement of *csrA* transcript levels in sRNAs overexpression strains. Even without IPTG-mediated induction of *csrB* and *csrC* expression, we found a higher level of *csrA*-encoding transcripts. We suggest that a yet unknown autoregulatory control circuit of the Csr system causes this feedback mechanism. However, previous studies by other research groups showed the successful inhibition of CsrA's activity by the sRNAs through phenotypical results and changes in downstream targets of CsrA.[16,17] Hence, the interdependency of the Csr components observed in the frame of this study deserves further investigation.

One of the advantages of the established *glgC-lux* luciferase reporter assay setup is for instance the direct readout of potential CsrA inhibition. Even though the regulation of the Csr system is complex and contains multiple feedback mechanisms, this *in bacterio* assay has a well-detectable and stable read-out in the presence of the natural antagonist CesT. That means once CsrA is less active (due to inhibition), we can directly monitor its consequence and impact through this assay. Thus, it is sensitive towards the activity of potential pathoblockers. In addition, quantitative evaluation of the cellular effect (determination of $EC_{50}$ values) of promising new inhibitors should be possible via concentration-dependent experiments as well as potentially gaining insights into the regulatory kinetics with the time-dependent measurement setup. Moreover, in combination with a qPCR expression gene assay, we can even observe the expression levels of different downstream targets of CsrA.

Downscaling of the required culture volume to 96-well format was successful enabling high throughput testing of potential inhibitors. Using this reporter gene assay set up for phenotypic screening from commercial synthetic or natural product libraries is highly favorable and is one of the next major steps towards tackling this challenging virulence-modulating target. The previously reported disruption of CsrA/RsmA-RNA interactions *in vitro* using the target protein from multiple species holds promise for the identification of anti-infectives/virulence modulators with broader anti-Gram-negative activity.[8]

## Experimental Section

### Bacterial strains and culture conditions

All strains and plasmids used in this study are described in the supplementary Table S2. Unless otherwise indicated, bacterial strains were routinely grown in LB medium at 37 °C containing the following antibiotics with respective final concentrations: ampicillin (100 μg/mL) and kanamycin (50 μg/mL).

### Luciferase reporter gene assay

*E. coli* (BL21, DH5alphα, MG1655) pvBE3 with respective plasmids of inducible genes was grown in different vessels ranging from 10 mL (in falcon tubes) to 100 mL (in shaking flasks) at 37 °C to exponential phase ($OD_{600}$ = 0.6). Subsequently, IPTG (500 μM) was added to induce the expression of CsrB, CsrC, or CesT. After 4 hours the cultures were added into the wells of a microtiter plate (200 μL per well) and luminescence (relative light units – RLU) was measured in triplicate. In addition to that, optical density (OD) at 600 nm was measured in 1 : 10 dilution.

### Time-dependent measurement

Flask and falcon tube format: *E. coli* BL21 pvBE3 and *E. coli* BL21 pvBE3 with an additional plasmid carrying the *cesT* gene were grown at 37 °C to exponential phase ($OD_{600}$ = 0.6). Subsequently, compound (500 μM; 250 μM; 125 μM, final concentrations) and DMSO (5 %) were added each to *E. coli* BL21 pvBE3. After 5 min the first measurement was performed (time point 5 min). The culture was added to the measuring plates (200 μL per well) and luminescence (relative light units – RLU) was determined in triplicate. Afterwards, measurements were done every hour via the same procedure. In addition to that, optical density (OD) at 600 nm was measured in 1 : 10 dilution.

Microtiterplate format: *E. coli* strains BL21 pvBE3 with or without the plasmid pNS6236 (cesT+) were grown at 37 °C until OD = 0,6 is reached. Afterwards, cultures were diluted in LB medium to OD = 0.06. 100 μL of diluted cultures were transferred into the 96-well plates preloaded with 100 μL LB and 5 % DMSO per well. (200 μL per well in total). The relative light units (RLU) and OD600 were determined directly from one plate every hour.

### Isolation of total RNA

The total amount of the cellular RNA from each culture was isolated using the RNeasy Mini Kit (Qiagen, Hilden, Germany) according to the manufacturer's protocol. To avoid DNA contaminations, DNA digestions were conducted with DNase (Qiagen, Hilden, Germany) for 15 min. RNA was quantified by its absorbance at 260 nm and 280 nm using NanoDrop™. RNA samples were stored at −20 °C for only one-time usage.

### Reverse transcription PCR (RT-PCR)

Reverse transcription was conducted using Applied Biosystems™ High-Capacity cDNA Reverse Transcription Kit (fisher scientific, USA). The reaction mixture (20 μL) contained 100 ng of RNA and master mix with reverse transcriptase. The conditions for the PCR were: 25 °C–10 min, 37 °C–120 min, 85 °C–5 min. cDNA products were either used directly for qPCR or stored at −20 °C.

### Quantitative PCR (qPCR)

The qPCR was performed using SYBR Green master mix (Thermofisher Scientific, Germany) and respective primers listed in the supplementary information (Table S3). The samples consisted of 10 μL master mix, 0,5 μL cDNA product, 7,5 μL $H_2O$ and 2 μL primers. Reactions for each sample were performed with StepOnePlus™ Real-Time PCR system (Thermofisher Scientific, Germany). The conditions for the qPCR were: 50 °C–2 min, 90 °C–2 min (holding stage), 95 °C–15 sec, 60 °C–1 min (40 cycles in the cycling stage), 95 °C–15 sec, 60 °C–1 min, 95 °C–15 sec (melt curve stage). The difference in cycle threshold (△CT) between control samples (wildtype MG1655, BL21 and DH5alpha strains) and treated samples (strains with plasmids containing inducible *csrB, csrC*, and *cesT* genes) was calculated using the Comparative Cτ (△△Cτ) Quantification method. Expression of individual genes was normalized against the *rpoD* and *opgD* genes. All the results were calculated and analyzed using Excel (Microsoft). The resulting values represent the mean expression level of duplicates from one qPCR assay.

## Supporting Information

The authors have cited additional references within the Supporting Information.[18–19]

## Acknowledgements

This work is supported by the Deutsche Forschungsgemeinschaft (DFG) through "RESIST - Resolving Infection Susceptibility" cluster of excellence (EXC 2155). We thank Prof. Dr. Ilan Rosenshine for sending us the *cesT*$^+$ plasmid pNS6236. We also thank Philipp Alexander Gansen and Dominik Kolling for their help and support. Open Access funding enabled and organized by Projekt DEAL.

## Conflict of Interests

The authors declare no conflict of interest.

## Data Availability Statement

The data that support the findings of this study are available in the supplementary material of this article.

**Keywords:** anti-infectives · carbon storage regulator A · reporter gene assay · repressor of secondary metabolites A · virulence modulation

[1] S. A Strathdee, S. C Davies, J. R Marcelin, *Lancet* **2020**, 1050–1052.
[2] E. Tacconelli, E. Carrara, A. Savoldi, S. Harbarth, M. Mendelson, D. L. Monnet, C. Pulcini, G. Kahlmeter, J. Kluytmans, Y. Carmeli, M. Ouellette, K. Outterson, J. Patel, M. Cavaleri, E. M. Cox, C. R. Houchens, M. L. Grayson, P. Hansen, N. Singh, U. Theuretzbacher, N. Magrini, A. O. Aboderin, S. S. Al-Abri, N. Awang Jalil, N. Benzonana, S. Bhattacharya, A. J. Brink, F. R. Burkert, O. Cars, G. Cornaglia, O. J. Dyar, A. W. Friedrich, A. C. Gales, S. Gandra, C. G. Giske, D. A. Goff, H. Goossens, T. Gottlieb, M. Guzman Blanco, W. Hryniewicz, D. Kattula, T. Jinks, S. S. Kanj, L. Kerr, M.-

P. Kieny, Y. S. Kim, R. S. Kozlov, J. Labarca, R. Laxminarayan, K. Leder, L. Leibovici, G. Levy-Hara, J. Littman, S. Malhotra-Kumar, V. Manchanda, L. Moja, B. Ndoye, A. Pan, D. L. Paterson, M. Paul, H. Qiu, P. Ramon-Pardo, J. Rodríguez-Baño, M. Sanguinetti, S. Sengupta, M. Sharland, M. Si-Mehand, L. L. Silver, W. Song, M. Steinbakk, J. Thomsen, G. E. Thwaites van der Meer, Jos WM, N. van Kinh, S. Vega, M. V. Villegas, A. Wechsler-Fördös, H. F. Wertheim, E. Wesangula, N. Woodford, F. O. Yilmaz, A. Zorzet, *The Lancet Infect. Dis.* **2018**, *18*, 318–327.
[3] A. L. Welp, J. M. Bomberger, *Front. Cell. Infect. Microbiol.* **2020**, *10*, 213.
[4] K. A. Brogden, J. M. Guthmiller, C. E. Taylor, *The Lancet* **2005**, *365*, 253–255.
[5] E. M. Selleck, M. S. Gilmore, *mBio* **2016**, *7*, 1–3.
[6] A. K. Heroven, K. Böhme, P. Dersch, *RNA Biol.* **2012**, *9*, 379–391.
[7] C. K. Maurer, M. Fruth, M. Empting, O. Avrutina, J. Hoßmann, S. Nadmid, J. Gorges, J. Herrmann, U. Kazmaier, P. Dersch, R. Müller, R. W. Hartmann, *Future Med. Chem.* **2016**, *8*, 931–947.
[8] V. Jakob, B. G. Zoller, J. Rinkes, Y. Wu, A. F. Kiefer, M. Hust, S. Polten, A. M. White, P. J. Harvey, T. Durek, D. J. Craik, A. Siebert, U. Kazmaier, M. Empting, *Eur. J. Med. Chem.* **2022**, *231*, 114148.
[9] T. Romeo, P. Babitzke, *Microbiol. Spectrum* **2018**, *6*, 1–13
[10] C. A. Vakulskas, A. H. Potts, P. Babitzke, B. M. Ahmer, T. Romeo, *Microbiol. Mol. Biol. Rev.* **2015**, *79*, 193–224.
[11] V. Berndt, M. Beckstette, M. Volk, P. Dersch, M. Broenstrup, *Sci. Rep.* **2019**, *9*, 1–15.
[12] T. Weilbacher, K. Suzuki, A. K. Dubey, X. Wang, S. Gudapaty, I. Morozov, C. S. Baker, D. Georgellis, P. Babitzke, T. Romeo, *Mol. Microbiol.* **2003**, *48*, 657–670.
[13] N. Katsowich, N. Elbaz, R. R. Pal, E. Mills, S. Kobi, T. Kahan, I. Rosenshine, *Science* **2017**, *355*, 735–739.
[14] M. Yadav, M. Srinivasan, N. K. Tulsian, Y. X. Liu, Q. Lin, I. Rosenshine, J. Sivaraman, *Protein Sci.* **2021**, *30*, 2433–2444.
[15] F. Uliczka, F. Pisano, A. Kochut, W. Opitz, K. Herbst, T. Stolz, P. Dersch, *PLoS One* **2011**, *6*, 1–12.
[16] Tony Romeo, *Mol. Microbiol.* **1998**, *29*, 1320–1330.
[17] A. E McKee, B. J Rutherford, D. C Chivian, E. K Baidoo, D. Juminaga, D. Kuo, P. I Benke, J. A Dietrich, S. M Ma, A. P Arkin, C. J Petzold, P. D Adams, J. D Keasling, S. R Chhabra, *Microb. Cell Fact.* **2012**, *11*, 1–12.
[18] H. Prochnow, V. Fetz, S.-K. Hotop, M. A. García-Rivera, A. Heumann, M. Brönstrup, *Anal. Chem.* **2019**, *91*, 1863–1872.
[19] V. R. Matias, A. Al-Amoudi, J. Dubochet, T. J. Beveridge, *J. Bacteriol.* **2003**, *185*, 6112–6118.

Manuscript received: May 17, 2023
Revised manuscript received: July 12, 2023
Accepted manuscript online: July 12, 2023
Version of record online: July 25, 2023